Journal of Integrative Agriculture 2026, 25(9): 3725–3735

Available online at ScienceDirect

Journal of Integrative Agriculture

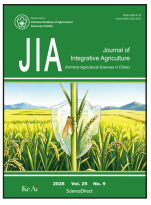

RESEARCH ARTICLE

The *Clygp* (*yellow-green plant*) encodes a signal recognition particle 54 kDa protein modulating chloroplast development and photosynthesis in watermelon

Shixiang Duan[1, 2*], Yaomiao Guo[1, 2*], Lin Deng[1, 2], Qishuai Kang[1, 2], Changbao Shen[1, 2], Xiaohang Xue[1, 2], Junling Dou[1, 2], Dongming Liu[1, 2], Sen Yang[1, 2], Xingping Zhang[4], Yun Deng[4], Huayu Zhu[1, 2#], Yongdong Sun[3#], Luming Yang[1, 2#]

[1] *College of Horticulture, Henan Agricultural University, Zhengzhou 450046, China*
[2] *Research Center of Cucurbit Germplasm Enhancement and Utilization of Henan Province, Zhengzhou 450046, China*
[3] *School of Horticulture and Landscape Architecture, Henan Institute of Science and Technology, Xinxiang 453003, China*
[4] *Peking University Institute of Advanced Agricultural Sciences, Weifang 261325, China*

Highlights

- A novel chlorophyll-deficient yellow-green mutant PKH352 was identified from an EMS-induced watermelon mutant library.
- Mutation in *ClG42_04g0106300* gene, encoding a signal recognition particle 54 kDa protein, leads to the yellow-green phenotype and reduced photosynthetic efficiency in watermelon.
- The *ClG42_04g0106300* gene plays an essential regulatory role in chloroplast biogenesis and chlorophyll metabolism in watermelon.

Abstract

Photosynthesis serves as the primary source of nutrients synthesized in higher plants, and improving photosynthetic efficiency can significantly increase crop yield and fruit quality. Leaf color mutants represent ideal materials for studying chloroplast development and photosynthesis mechanisms and have been widely characterized in field crops. However, relevant research on watermelon leaf color mutants remains scarce. In this study, we isolated a yellow-green phenotype mutant, PKH352, from an EMS-mutagenized watermelon mutant library. The chlorophyll content and maximal photochemical efficiency in PKH352 were significantly decreased. Genetic analysis showed that the mutated trait was controlled by a single nuclear gene, which was named *Clygp* (*Citrullus lanatus yellow-green plant*). Through MutMap and linkage analysis in an F_2 population of 440 plants, we identified a single nucleotide polymorphism (SNP) mutation within *ClG42_04g0106300*, which encoded a signal recognition particle 54 kDa protein, as the causal variant for the yellow-green phenotype. Further validation using a CRISPR/Cas9-mediated system confirmed that knockout of *ClG42_04g0106300* results in the yellow-green phenotype in watermelon. In addition, comparative transcriptomic analysis revealed that mutations in *ClG42_04g0106300* greatly affected the expression of key genes associated with chloroplast development and photosynthesis, providing strong evidence that this gene plays a critical role in these biological pathways. Taken together, these findings provide insights into the molecular mechanisms underlying chloroplast development and photosynthetic efficiency, offering a theoretical basis for breeding watermelon varieties with high photosynthetic efficiency.

Keywords: watermelon, yellow-green phenotype, photosynthesis, fine-mapping, gene editing

Received 19 April 2025; Received in revised form 4 July 2025; Accepted 29 August 2025; Available online 13 November 2025
Shixiang Duan, E-mail: sxiangduan@163.com; Yaomiao Guo, E-mail: yaomiaoguo@163.com; #Correspondence Huayu Zhu, E-mail: hyzhu@henau.edu.cn; Yongdong Sun, E-mail: sunyd2001@163.com; Luming Yang, E-mail: lumingyang@henau.edu.cn
* These authors contributed equally to this study.

doi: 10.1016/j.jia.2025.11.013

1. Introduction

In higher plants, photosynthesis serves as the primary source of nutrients, accounting for over 90% of the total biomass yield. Improving the level of photosynthetic efficiency can significantly enhance overall crop productivity (Wang F L *et al.* 2018; Wang *et al.* 2019; Croce *et al.* 2024). Leaf color mutants, particularly yellowing mutants, have become ideal materials for studying photosynthesis mechanisms and chloroplast biosynthesis due to their defects in chloroplast development or photosynthetic capacity (Zhao *et al.* 2020). Recently, numerous genes controlling leaf color mutants have been reported in field crops. To date, over 250 genes or QTL loci associated with leaf color have been identified in maize and rice, respectively (Wang F *et al.* 2018; Li W R *et al.* 2022), in which most of them impact chloroplast development and photosynthetic efficiency. For example, the *ZmYL412* gene encodes glutamyl-tRNA reductase, and mutations in this gene lead to a decrease in chloroplast number and a reduction in net photosynthetic efficiency in maize (Yang W Z *et al.* 2023). Similarly, the rice nuclear-encoded chloroplast protein YL1 participates in the biosynthesis of chloroplast ATPase complexes through interaction with the ATP β subunit. Deficiency in YL1 disrupts the expression of genes related to chloroplast development and photosynthesis (Chen *et al.* 2016).

Chlorophyll, the main photosynthetic pigment in higher plants (Cackett *et al.* 2021), binds to light-harvesting proteins on the thylakoid membrane of chloroplasts (Zhang *et al.* 2023). It is responsible for capturing light energy during photosynthesis and driving electron transfer in the photosynthetic reaction center (Lan *et al.* 2022; Li *et al.* 2025). The efficiency of plant photosynthesis depends on the absorption and conversion of solar energy by chlorophyll and chlorophyll-binding proteins (Cardona *et al.* 2018). Among these proteins, light-harvesting complex proteins (LHCs) are key light-harvesting protein, constituting up to 50% of the thylakoid membrane proteins (Levin and Schuster 2023). After synthesis on cytoplasmic ribosomes, LHCs are transported into chloroplasts through the TOC/TIC translocation machinery of the chloroplast envelope and translated into precursor proteins. These precursors form a transport complex with the chloroplast signal recognition particle (cpSRP) complex for delivery to the thylakoid membrane. The cpSRP complex is a heterodimer composed of cpSRP54 and the chloroplast-specific cpSRP43 (Schünemann 2004; Kirst and Melis 2014). It is formed through the interaction between the C-terminus of cpSRP54 and the CD2 domain of cpSRP43 (Hristou *et al.* 2019; Bischoff *et al.* 2024). cpSRP43 binds directly to LHCs, while cpSRP54 promotes structural rearrangement within cpSRP43, enhancing its affinity for LHCs and facilitating its binding. Additionally, cpSRP54 interacts with FtsY, which assists in targeting the LHCs complex to the thylakoid membrane. Thus, cpSRP54 plays a crucial role in the transport of LHCs. When the absence of cpSRP54 and cpFtsY, cpSRP43 can still mediate LHCs transport, but with significantly reduced efficiency (Walter *et al.* 2015; Ji *et al.* 2021).

Watermelon (*Citrullus lanatus*), a member of the Cucurbitaceae family, is one of the top ten fruits globally. Its yield and quality are directly linked to the economic interests of cultivators. Photosynthesis as a critical factor influencing yield and quality, making the study of photosynthetic mechanisms in watermelon highly important. Leaf color mutants serve as ideal materials for studying photosynthesis. However, research on leaf color mutants in watermelon remains limited, and only a few genes controlling these traits have been mapped and cloned. To date, only two genes associated with leaf color mutations have been reported. Zhu *et al.* (2022) conducted hybridization between the yellow watermelon mutant *w-yl* and the inbred line ZK. The *w-yl* gene was mapped to a 2.217 Mb region on chromosome 2, with *Cla97C02G036040*, *Cla97C02G036050*, and *Cla97C02G036060* were identified as potential candidates responsible for the yellowing phenotype. Gebremeskel *et al.* (2023) mapped the *dg* gene to a 53.54 kb region on chromosome 3 using bulk segregant analysis and linkage analysis based on a delayed green mutant. And the *ClCG03G010030* gene, encoding an FtsH extracellular protease family protein, was proven to be involved in the early development of delayed green leaves. Despite these findings, the currently identified genes cannot meet the needs of studying the photosynthesis mechanism of watermelon and conducting high-efficiency watermelon breeding. Therefore, further study on leaf color mutants and the cloning of additional target genes are essential to advance our understanding of photosynthesis and improve watermelon breeding strategies.

In this study, we identified a novel chlorophyll-deficient mutant, PKH352, from an ethyl methanesulfonate (EMS) mutagenized population of the cultivar G42. PKH352 exhibits yellow-green coloration in its above-ground organs, accompanied by reduced chlorophyll content and lower maximal photochemical efficiency. Genetic analysis revealed that the phenotype is controlled by a single recessive gene, *Clygp*. MutMap and linkage analysis identified *ClG42_04g0106300* as the candidate gene for *Clygp*, which encodes a signal recognition particle 54 kDa protein (cpSRP54). A SNP mutation in its coding sequence leads to a truncated protein, resulting in the yellow-green phenotype in watermelon. This was further validated by knockout of *ClG42_04g0106300* in watermelon. Additionally, transcriptomic profiling (RNA-seq) demonstrated that *ClG42_04g0106300* participates in regulating chloroplast development and photosynthetic pathways. Collectively, these findings identify *ClG42_04g0106300* as a critical regulator of photosynthesis machinery and provide insights into chloroplast biogenesis. These findings enhance our understanding of the molecular mechanisms underlying photosynthesis and provide a foundation for high photosynthesis-efficiency breeding in watermelon.

2. Materials and methods

2.1. Genetic population construction and planting

The leaf color mutant PKH352 was generated by treating pollen of the watermelon inbred line G42 with EMS (Deng *et al.* 2022). G42 exhibits normal green in all aboveground organs, while PKH352 displays yellow-green color in the

aboveground organs throughout the entire growth period. The F_1 generation was obtained by crossing G42 and PKH352, and a segregating F_2 population was generated through self-crossing. All materials were sown in 50-hole trays and transplanted to the greenhouse at Maozhuang Research Station of Henan Agricultural University (Zhengzhou, China).

The leaf color phenotype was assessed at the seedling stage, 30 and 60 d after planting, respectively. The χ^2-test was used to evaluate deviations of the observed leaf color phenotype data in the F_2 population from the theoretically expected segregation ratio.

2.2. Chlorophyll, carotenoid and chlorophyll fluorescence dynamic parameters analyses

The contents of chlorophyll and carotenoids were measured using spectrophotometry. Fresh leaves were collected from the 10th node of the tested materials at 30 d after planting, and 0.2 g of each sample was suspended in 95% ethanol (Boxiang Biotechnology, Zhengzhou, China). After incubation in the dark for 48 h, 200 μL of the extraction solution was taken and measured using a spectrophotometer at wavelengths of 665, 649, and 470 nm (Shanghai Yitian Precision Instrument, Shanghai, China). The chlorophyll and carotenoid contents were calculated according to the method described by Lichtenthaler (1987).

Chlorophyll fluorescence kinetics (F_v/F_m) were measured using a pulse-modulated fluorometer (WALZ, Free State of Bavaria, Germany). Leaves were collected from the 10th node of the tested materials of 30 d after planting and dark-adapted for 30 min. The ground state fluorescence (F_o) was measured, followed by exposure to saturated pulsed light to determine the maximum fluorescence (F_m). The F_v/F_m ratio was calculated using the formula: $F_v/F_m=(F_v/F_m–F_o)/F_m$. At least three individual plants were used for each experiment.

2.3. Transmission electron microscopy (TEM)

Fresh leaves from the tested materials were cut into 3 mm×3 mm sections. These sections were fixed with 2.5% glutaraldehyde at 4°C for 4 h. Then, fixed with 1.0% osmium tetroxide at 4°C for 1.5 h. The samples were dehydrated using a graded ethanol series (50%–90%) and acetone (90%) and embedded in resin (Boxiang Biotechnology, Zhengzhou, China). Finally, the samples were stained with 2% uranyl acetate and lead citrate trihydrate. Ultrathin sections were prepared using an ultramicrotome and viewed using a Hitachi HT7700 transmission electron microscope (FEI, State of Oregon, USA).

2.4. Genomic resequencing and MutMap analysis

The mutant DNA pool was constructed by mixing DNA from 25 randomly selected yellow-green phenotype plants from the F_2 segregating population as previously described (Zhu *et al.* 2019; Liu *et al.* 2025). The wild-type DNA pool was constructed using DNA from the wild-type material G42. Genome resequencing of the two DNA pools was performed following the standard Illumina protocol, and paired-end sequencing was conducted on the Illumina HiSeq 2500 platform. The sequencing depth for both libraries was no less than 50× (Biomarker Technologies, Beijing, China).

The resequencing data were filtered using Fastp to remove short reads and low-quality reads. The resulting clean reads were mapped to the watermelon reference genome 'G42' (watermelondb.cn) using software BWA. To identified the chromosome region of candidate target genes using MutMap software (Fekih *et al.* 2013), and the Δ(SNP-index) graph was generated using the ggplot2 package in R.

2.5. Marker development and linkage analysis

The resequencing data from the mutant pool and G42 were aligned to chromosome 4 of the watermelon reference genome 'G42' using BWA, and mutation sites were identified using GATK. SNPs showing differences between the mutant pool and G42 were then designed into dCAPS markers using dCAPS Finder 2.0 software (Neff *et al.* 2002) (Appendix A).

PCR amplifcation of molecular markers and subsequent gel electrophoresis were conducted as previously described (Dou *et al.* 2022). Linkage analysis was performed with the Kosambi mapping function in JoinMap 5.0, using the threshold logarithm 10 of the odds (LOD) score of 5.0 (Duan *et al.* 2023).

2.6. Subcellular localization

The CDS sequence of *ClG42_04g0106300* without a stop codon from G42 and inserting into the *Sma*I and *Spe*I sites of the pCAMBIAI1300 vector using homologous recombination. The plasmid pCAMBIAI1300-35S-ClYGP-GFP was constructed and transformed into Agrobacterium GV3101 and then infiltrated into tobacco leaves. The pCAMBIA1300-35S-GFP vector was used as a control. After 1 d of dark treatment and 1 d of light treatment, the green fluorescent protein signals in the tobacco epidermal cells were examined using an LSM700 confocal laser scanning microscope (Nikon, Tokyo Metropolis, Japan).

2.7. RT-qPCR analysis

Total RNA was extracted from different tissues (roots, stems, male flowers, ovaries, leaves) of PKH352 and G42 at 30 d after planting. cDNA was synthesized using the reverse transcriptase (Vazyme, Nanjing, China). The qRT-PCR of genes were performed using SYBR® *Premix Ex Taq* (TaKaRa Bio, Tokyo Metropolis, Japan). Experiments from conducted with three biological and technical replicates, and the data were analyzed using the $2^{-\Delta\Delta CT}$ method. Primers of genes for qRT-PCR were designed based on Cucurbitaceae Genome Database (http://cucurbitgenomics.org/) and NCBI web (https://blast.ncbi.nlm.nih.gov/Blast.cgi) (Yang *et al.* 2022).

2.8. Watermelon genetic transformation

The knockout lines of *ClYGP* in watermelon were generated using CRISPR/Cas9 system. The CRISPR/Cas9 vector construction and transformation were performed following previously described methods (Niu *et al.* 2024). Two single guide RNAs (sgRNAs) binding sites in the exon of *ClYGP* were designed by CRISPR design software (https://crispr.dbcls.jp/) (Naito *et al.* 2015). The transformation assay was conducted using watermelon inbred lines YL. Positive plants were screened using a handheld fluorescence analyzer, and confirming the editing form through Sanger sequencing.

2.9. RNA-seq analysis

The leaves from the 10th node of G42 and PKH352 were collected at 30 d after planting to construct RNA-seq library, separately. Three biological replicates were performed for each material (Liu *et al.* 2020). The RNA-seq libraries were sequenced on an Illumina HiSeqTM 4000 platform (Biomarker Technologies, Beijing, China). The adaptor sequences containing N and low-quality reads were filtered and removed using Fastp, and the clean reads were mapped to the watermelon reference genome use hisat2, and the read numbers of annotated genes were counted by featureCounts. DEGs between PKH352 and G42 were identified using the DESeq2 package in R with a corrected *P*-adjust<0.05. The DEGs were validated in the leaves of PKH352 and G42 using RT-qPCR. GO and KEGG functional enrichment analysis of the common differentially expressed genes was performed using TBtools software (Chen *et al.* 2020). The GO and KEGG enrichment results were visualized through the online website Weishengxin (Tang *et al.* 2023).

3. Results

3.1. Phenotypic and genetic analysis of yellow-green mutant PKH352

We identified a chlorophyll-deficient mutant, PKH352, from an EMS mutagenesis library of watermelon inbred line G42. This mutant exhibited yellow-green color in its aboveground organs throughout the entire growth cycle. Furthermore, the PKH352 mutant was slightly smaller than G42, producing smaller fruits with a lighter green skin color (Fig. 1-A, B and H). Compared to the wild-type G42, the mutant PKH352 showed significantly lower levels of chlorophyll (–59%) and carotenoid (–40%) content (Fig. 1-I), as well as a 28% reduction in the maximal photochemical efficiency (F_v/F_m) (Fig. 1-C and J). These results suggest that the reduced pigment content in PKH352 leads to significant impairment of its photosynthetic capacity. To further investigate the cytological structure for the decreased pigment content in PKH352, we observed the morphology and number of chloroplasts in mesophyll cells from G42 and PKH352 using transmission electron microscopy. The results showed that the chloroplasts in G42 were evenly distributed and exhibited normal development. In contrast, the chloroplasts in PKH352 displayed structural abnormalities, including a distorted thylakoid membrane system and a significantly lower number of chloroplasts (Fig. 1-D–G and K).

To genetically characterize the yellow-green phenotype in PKH352, we crossed PKH352 with G42 to generate F_1 plants. All F_1 plants exhibited a normal green phenotype similar to G42. Subsequently, the F_2 generation was produced by self-crossing of F_1 plants. Among 440 F_2 plants, 332 displayed a green phenotype, while 108 exhibited a yellow-green

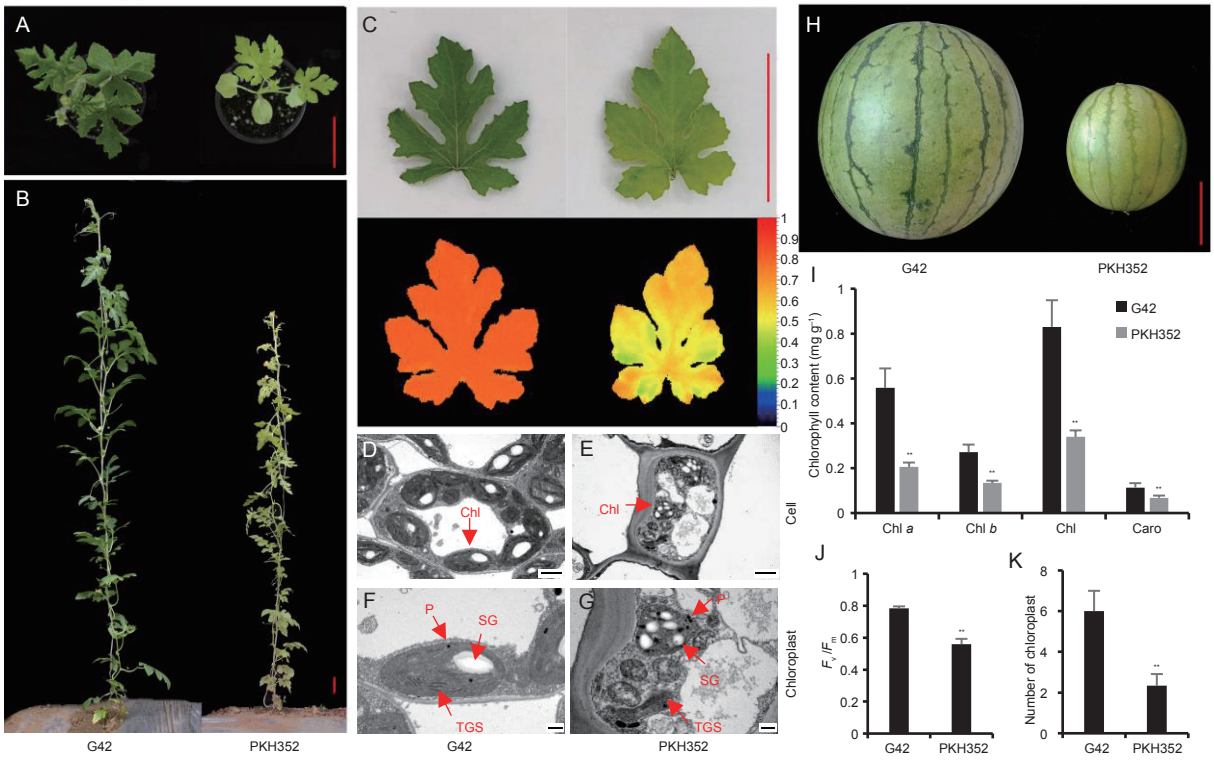

Fig. 1 Phenotype characterization of the wild-type G42 and PKH352 mutant plants. A and B, phenotypes of G42 and PKH352 at 15 and 45 d after seeding. Scale bars, 5 cm. C, images showing the maximal photochemical efficiency (F_v/F_m) from G42 and PKH352. Scale bars, 5 cm. D–G, transmission electron micrographs of leaves from G42 and PKH352. Chl, chloroplast; P, osmiophilic granules; SG, starch grains; TGS, thylakoid granum stacks. Cell Scale bars, 2 μm. Choroplast scale bars, 500 nm. H, fruits from G42 and PKH352. Scale bars, 5 cm. I, chlorophyll and carotenoid content of leaves from G42 and PKH352. J, comparison of the maximal photochemical efficiency (F_v/F_m) of leaves between G42 and PKH352. K, comparison of chloroplast number of per leaf cell between G42 and PKH352. Data were shown as means±SD (*n*=3). **, *P*-value<0.01.

phenotype, which fit to a segregation ratio of 3:1, indicating that the yellow-green phenotype in PKH352 is controlled by a single recessive gene (Appendix B). We designated this causal locus as *Clygp*.

3.2. Fine mapping of the *Clygp* gene

To rapidly map the *Clygp* locus, MutMap analysis was performed mapping through the F_2 population. We selected 25 plants with the yellow-green phenotype at random from the F_2 population for pooling into mutant pool. Genomic DNA from the mutant pool and the wild-type parental lines G42 were used for paired-end library construction and next-generation sequencing. Each library was sequenced at a depth of 50× genome coverage. A total of 38.86 Gb of clean data were generated and mapped to the watermelon reference genome 'G42', with over 95% of short reads successfully aligned (Appendix C). A total of 9,441 SNPs and InDels were detected. To further identify the genomic region associated with the *Clygp* locus, we analyzed the Δ(SNP-index) values between the mutant pool and G42. The results revealed a significant peak on the terminal region of chromosome 4, which exceeded the threshold value and approached 1.00 (Fig. 2-A).

To fine-map the *Clygp* locus, we designed dCAPS molecular markers based on identified SNP loci around the peak region. A total of four dCAPS markers were designed to construct linkage map for *Clygp* in a small F_2 population containing 140 plants. The *Clygp* locus was mapped between dCAPS2 and dCAPS3, defining a candidate region of 1.89 Mb (24,027,844 –25,921,902). Within this region, only one SNP (24,866,058: G>A) was identified as differing between the mutant pool and the G42. Based on this SNP, dCAPS5 was developed and shown to co-segregate with the yellow-green phenotype in the small F_2 population (Fig. 2-B). Further genotyping of all F_2 plants using dCAPS5 confirmed its complete co-segregation with the yellow-green phenotype (Appendix D). These results suggest that this SNP is the causal mutation underlying the yellow-green phenotype in PKH352.

According to the annotation of the watermelon reference genome, the SNP (24866058) was located in the coding sequence of *ClG42_04g0106300*. The full length of *ClG42_04g0106300* is 6,705 bp, consisting of 15 exons. The single nucleotide substitution from C to T at the base 6,191 in the 13th exon introduced a premature stop codon, leading to a truncated protein with a loss of 85 amino acids (Fig. 2-C; Appendix E). These results suggest that the *ClG42_04g0106300* is the candidate gene of *Clygp*.

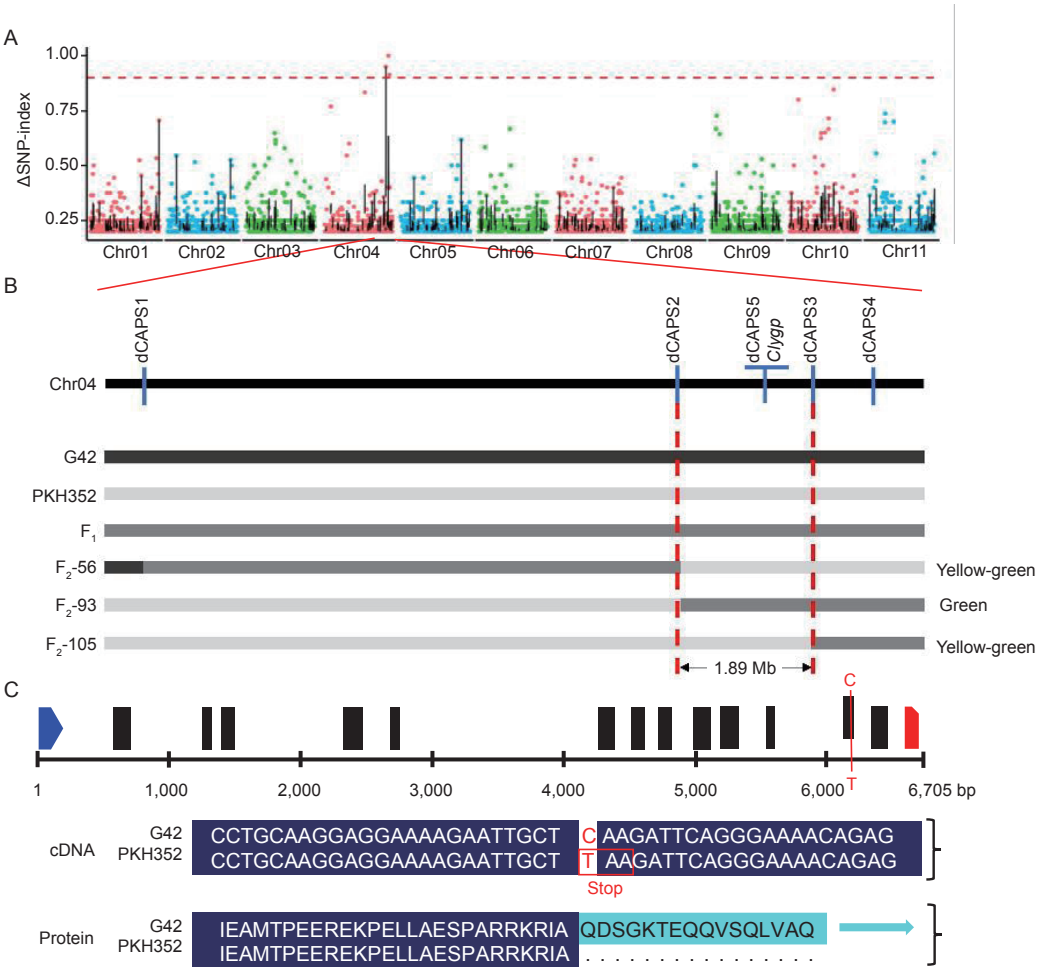

Fig. 2 Positional cloning and sequence alignment of the *Clygp* gene. A, Δ(SNP-index) graph of Mutmap analysis. B, genetic mapping of the *Clygp* gene. C, genomic structure of the candidate gene *ClG42_04g0106300* and its sequence alignment between PKH352 and G42.

3.3. Analysis of the *ClYGP* in watermelon

The *ClYGP* gene encodes cpSRP54 protein. According to previous studies, cpSRP54 binds to the chloroplast-specific protein cpSRP43 to form a complex, which mediates the targeting of light-harvesting complex (LHC) proteins to the thylakoid membrane. To better understand the genetic and functional conservation of cpSRP54 across species. We conducted a BLAST analysis to identify homologous proteins in various crop species, including model crops (*Arabidopsis*), field crops (maize, rice, wheat, soybean), and horticultural crops (tomato, cucumber, and melon), using the amino acid sequence of *ClYGP* (Appendix F). Amino acid sequence alignment revealed that all homologous genes exhibit high similarity and include the same structural domain (Appendix G). Phylogenetic analysis revealed that the ortholog genes of all monocotyledons are clustered together, while the ortholog genes of dicotyledons are located in an outer branch. The highest similarity of orthologs in watermelon, melon, and cucumber is concentrated in the same small branch, and all are single-copy genes (Fig. 3-C). In *Arabidopsis*, the homolog of *ClYGP*, *AT5G03940*, is essential for chloroplast development. Mutations in *AT5G03940* result in impaired chloroplast development and pale-green leaves. This suggested that ClYGP might have similar functions to that of other cpSRP54 proteins in watermelon.

To clarify the expression pattern of *ClYGP* in watermelon, we analyzed its expression levels in different tissues of PKH352 and G42 using qRT-PCR. *ClYGP* was highly expressed in leaves and fruits, with higher expression levels in G42 compared to PKH352 across all tissues (Fig. 3-A). Furthermore, to determine the subcellular localization of ClYGP, we constructed its full-length CDS into a 1300 subcellular localization vector and transiently expressed it in tobacco mesophyll cells. Under confocal microscopy, the GFP fluorescence of ClYGP overlapped with chlorophyll autofluorescence, confirming localization of the ClYGP protein in chloroplasts (Fig. 3-B). These findings suggest that *ClYGP* plays a significant role in chloroplast-related functions in watermelon.

3.4. Functional validation of the *ClYGP* gene

To further verify if the *ClYGP* is the causal gene controlling the yellow-green phenotype in watermelon, we designed two target sites within the 3rd and 4th exons of *ClYGP* and employed the CRISPR/Cas9 system to knock out the gene in the wild-type YL background. Fortunately, we successfully obtained two homozygous knockout lines with distinct edited genotypes. The CR-1 line carried a 34 bp deletion at target 1, while the CR-2 line had a 195 bp deletion between target 1 and target 2. These mutations resulted in truncated proteins of 116 and 115 amino acids in CR-1 and CR-2, respectively (Fig. 4-A).

Both the CR-1 and CR-2 lines exhibited a yellow-green phenotype in aboveground organs, similar to the PKH352 mutant (Fig. 4-B). They showed significantly lower chlorophyll content (CR-1: –51%, CR-2: –58%) and reduced maximal photochemical efficiency (F_v/F_m) (CR-1: –24%, CR-2: –25%) compared to the control plants (Fig. 4-C, J and K). Furthermore, transmission electron microscopy of leaves revealed a significant decrease in chloroplast number and compromised thylakoid membranes in the knockout lines (Fig. 4-D-I and L). These results demonstrate that *ClYGP* affects chlorophyll accumulation in watermelon by regulating chloroplast development, further confirming that *Clygp* is the causal gene controlling the yellow-green phenotype in watermelon.

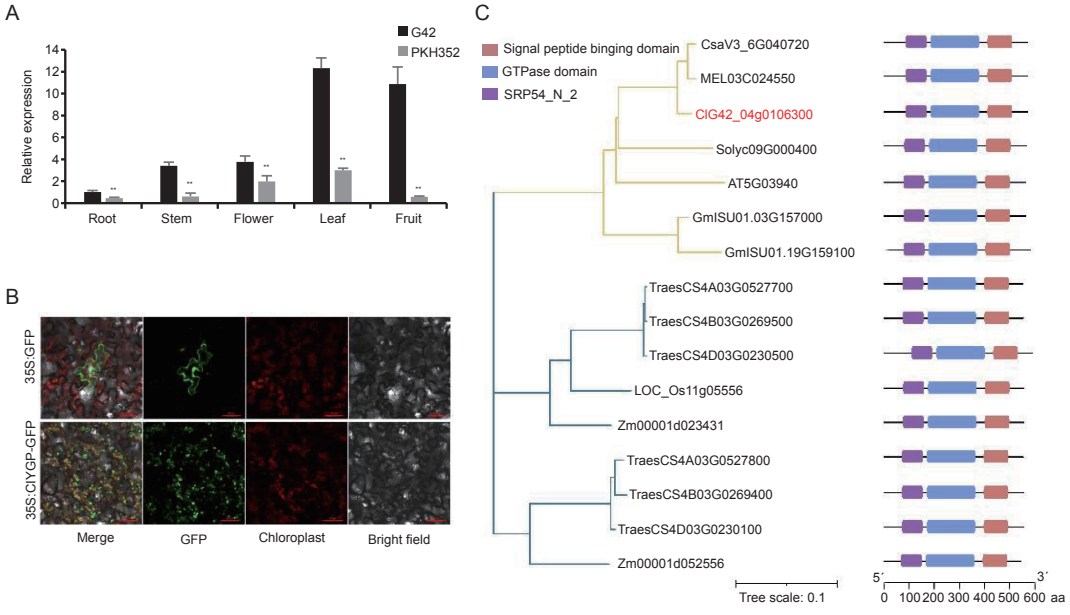

Fig. 3 Expression pattern and phylogenetic analysis of the *ClG42_04g0106300* gene. A, qRT-PCR analysis of *ClYGP* expression in different tissues from PKH352 and G42. B, subcellular localization of the ClYGP protein. C, phylogenetic tree of the ClYGP protein with the homologous proteins from other plant species. The blue branch denotes monocotyledonous plants, whereas the yellow branch denotes dicotyledonous plants.

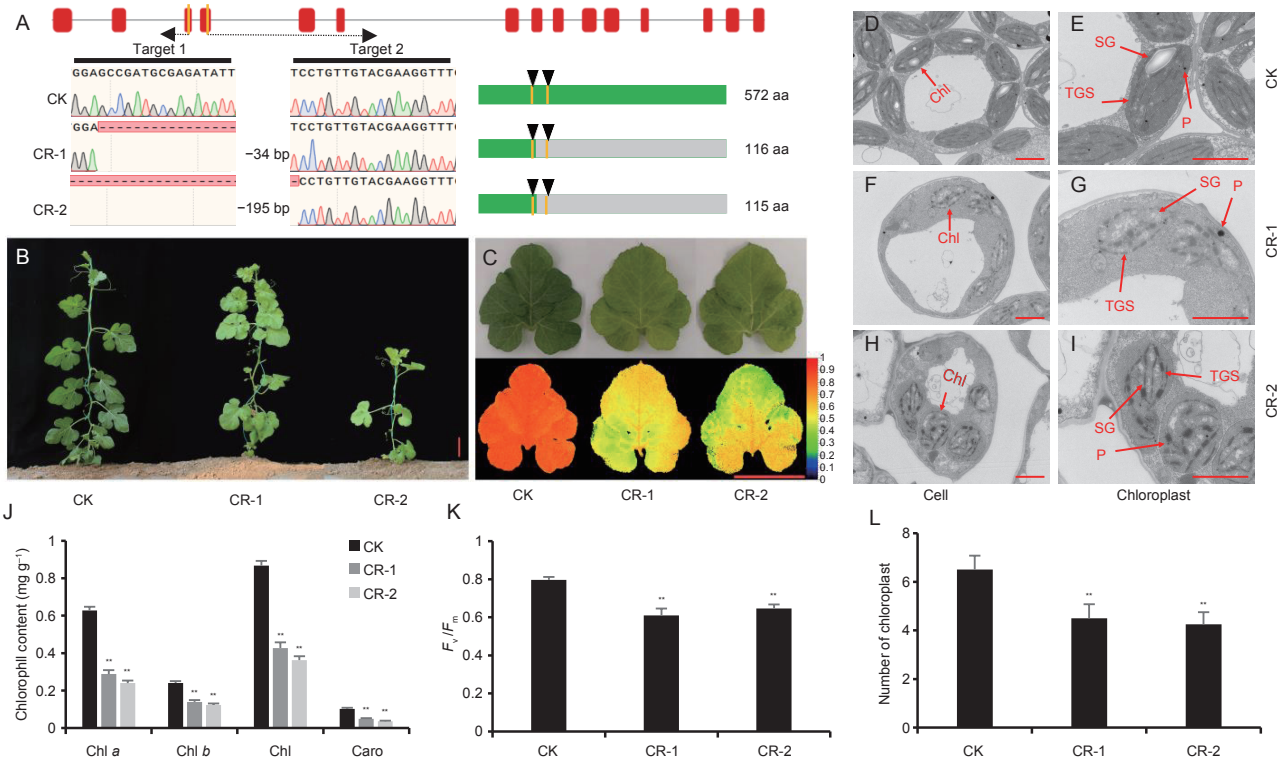

Fig. 4 Phenotypic characterization of *ClYGP* gene knockout lines and wild-type plants. A, mutation types in two *ClYGP* knockout lines. B, phenotypes. Scale bars, 5 cm. C, images showing the maximal photochemical efficiency (F_v/F_m). Scale bars, 5 cm. D–I, transmission electron micrographs of leaves. Chl, chloroplast; P, osmiophilic granules; SG, starch grains; TGS, thylakoid granum stacks. Scale bars, 2 μm. J, chlorophyll and carotenoid contents of leaves. K, comparison of F_v/F_m of leaves. L, chloroplast number of per leaf cell. Data were shown as means±SD (n=3). **, P-value<0.01.

3.5. Transcriptomic analysis of *ClYGP* regulated yellow-green phenotype in watermelon

To understand the molecular mechanism by which the *ClYGP* gene regulates yellow-green phenotype in watermelon, we performed transcriptome sequencing on leaves of PKH352 and G42, with three biological replicates per group. A total of 41.96 Gb of clean data was obtained, with an average of 6.99 Gb per sample. The alignment rate of all samples to the reference genome exceeded 94% (Appendix C). PCA showed high reproducibility among the biological replicates and significant differences between the two groups (Fig. 5-A).

Analysis of annotated gene expression levels revealed 1,924 differentially expressed genes (DEGs) in PKH352 compared to G42, including 1,165 up-regulated and 759 down-regulated genes (Fig. 5-B; Appendix H). Gene Ontology (GO) and Kyoto Encyclopedia of Genes and Genomes (KEGG) enrichment analyses indicated that the majority of DEGs were associated with chlorophyll synthesis and thylakoid development. Additionally, the DEGs were enriched in pathways related to Pentose phosphate pathway, Citrate cycle (TCA cycle), and photosystem functions. Specifically, KEGG enrichment analysis highlighted pathways such as Pentose phosphate pathway and Citrate cycle (TCA cycle) (Fig. 5-C). GO enrichment analysis showed that the cellular component category included chloroplast (GO:0009840) and thylakoid (GO:0031977), and the biological process category involved chloroplast rRNA processing (GO:1901259), thylakoid membrane organization (GO:0010027), and photosystem assembly (GO:0048564 and GO:0010207) (Fig. 5-D; Appendix I).

We further analyzed DEGs involved in chloroplast development and photosynthesis. Genes encoding zinc metalloproteases EGY1 and EGY2 (related to chloroplast development) and ATP-dependent zinc metalloproteases FTSH2 and FTSH12 (related to thylakoids) were upregulated in the mutant. Additionally, light-harvesting complex proteins (LHCA, LHCB, and LHCP), which are involved in light harvesting, were also upregulated. Conversely, transcription factors such as MYB and APRR2, which regulate chlorophyll biosynthesis, and chloroplastic-like FAD5 were downregulated in the mutant. Furthermore, the target gene, *ClG42_04g0106300*, was significantly downregulated in the transcriptome (Fig. 5-E). The expression patterns of these genes were further validated by qRT-PCR, confirming consistency with the transcriptome data (Fig. 6). These results demonstrate that *ClYGP* is required for efficient translational targeting of several central photosynthetic proteins. It plays a critical role in regulating chloroplast development and photosynthesis-related pathway genes.

4. Discussion

4.1. Identification and map-based cloning of a novel leaf color mutant in watermelon

Leaf color mutants not only affect chlorophyll content but

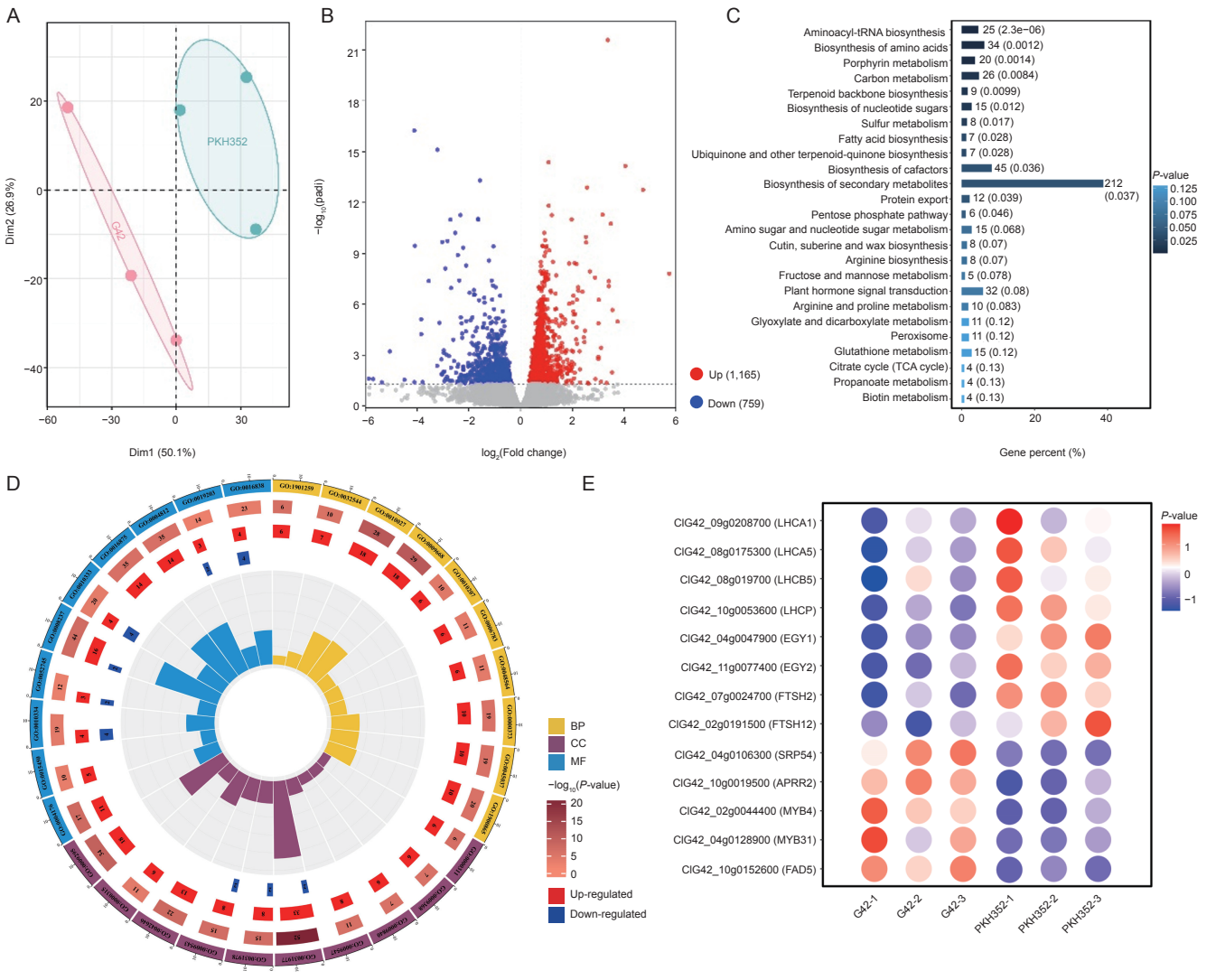

Fig. 5 Transcriptomic analysis of leaves from PKH352 and G42. A, principal component analysis of each sample. B, differentially expressed genes (DEGs) between PKH352 and G42. C, Kyoto Encyclopedia of Genes and Genomes (KEGG) enrichment analysis of DEGs. D, Gene Ontology (GO) enrichment analysis of DEGs. E, heatmap of genes related to chloroplast development among DEGs.

also influence photosynthetic capacity, making them ideal materials for studying photosynthesis mechanisms and chloroplast biosynthesis (Li Q L *et al.* 2022). In-depth research on leaf color mutants can facilitate the breeding of varieties with high photosynthetic efficiency (Zhang *et al.* 2021; Cutolo *et al.* 2023). In recent years, many leaf color mutants have been identified, and their target genes have been cloned in various species (He *et al.* 2023; Ma *et al.* 2023; Lu *et al.* 2024; Pan *et al.* 2024). Although leaf color mutants are common in nature, reports on naturally occurring leaf color mutants in watermelon are scarce. To date, only two mutants, *w-yl* and *dg*, have undergone gene mapping (Zhu *et al.* 2022; Gebremeskel *et al.* 2023).

In this study, we identified a yellow-green phenotype mutant, PKH352, from the M2 generation of EMS-mutagenized watermelon cultivar line G42. Phenotypic analysis showed that PKH352 is a chlorophyll-deficient mutant with reduced photosynthetic capacity. Cytological analysis revealed that the primary cause of the phenotype is incomplete chloroplast development and a reduced number of chloroplasts (Fig. 1). This observation is similar to the yellow-green plant mutant, NSL73046, in melon and the yellow leaf mutant, *yyl-1*, in cucumber (Hu *et al.* 2020; Yang S *et al.* 2023). Genetic analysis of the F_2 population derived from crossing PKH352 and G42 revealed that the yellow-green phenotype in PKH352 is controlled by a recessive mutated nuclear gene, *Clygp*. MutMap and linking analysis demonstrated that *ClG42_04g0106300*, encoding signal recognition particle 54 kDa protein (cpSRP54), is the target gene for *Clygp* (Fig. 2). A SNP (C>T) mutation in the encoding sequence, causing premature termination of amino acid translation, is responsible for the yellow-green leaf phenotype in PKH352, which has been further validated through CRISPR-Cas9-mediated gene editing in watermelon. A dCAPS marker was development base on this SNP showed complete co-segregation with the yellow-green plants in F_2 population (Appendix D), which will be highly useful in marker-assisted selection as the basis for genome selection breeding in watermelon.

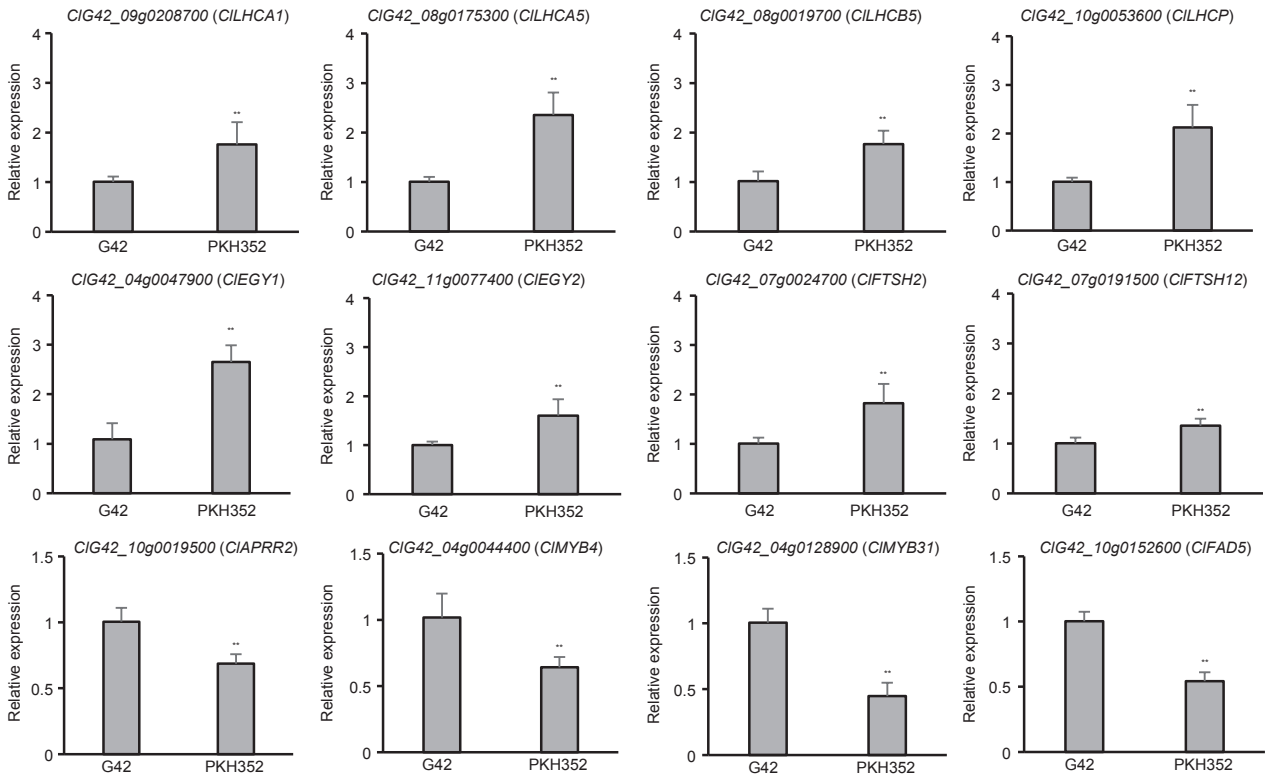

Fig. 6 RNA-seq results were validated using qRT-PCR.

4.2. The C-terminal structure of cpSRP54 is essential for its function

Conserved domains in genes are particularly important for maintaining gene function. These domains often serve as critical regions for protein–protein or protein–molecule interactions, ensuring the stability and efficiency of complex biological processes and signal transduction networks within organisms (Rocha *et al.* 2023). Mutations in the conserved regions of coding genes frequently have significant impacts on gene function. For example, a C>T point mutation in the *BrFLS* gene results in truncation of the BrFLS protein and the loss of the C-terminal conserved 2OG-FeII_Oxy functional domain, leading to abnormal anthocyanin accumulation in Chinese cabbage (Yue *et al.* 2024). In rice, the adaxial curled leaf mutant *cul1-1* is caused by a single base pair substitution (G>A) at 612 bp in exon 5. This mutation disrupts the conserved Chromo I domain of the CHD protein (Yang *et al.* 2025). In this study, amino acid sequence comparison between *Clygp* and its homologous genes in other species revealed that all homologs contain conserved NG structures and unique C-terminal structures (Appendix G).

In *Arabidopsis thaliana*, the yellow-green mutant *pga* is caused by a single SNP (G>A) mutation in the cpSRP54 gene, resulting in a nonsense mutation at the 89th amino acid residue of the cpSRP54 protein. This mutation results in the loss of 475 amino acids, disrupting the NG domain and the unique C-terminal structure (Lei *et al.* 2023). Although the yellow-green mutant PKH352 is also caused by a single SNP mutation in cpSRP54, Notable, The SNP (C>T) occurs at the end of the coding sequence and causes the 488th amino acid to be converted into a stop codon. As a result, the cpSRP54 protein in PKH352 loses only 85 amino acids at the C-terminus. This truncation affects only the unique C-terminal structure but does not disrupt the preceding NG domain (Appendix E). Although the two mutations have different effects on the structure of the cpSRP54 protein, both the PKH352 and *pga* mutants exhibit the same yellowing phenotype. In summary, it is suggested that the C-terminal structure of SRP54 play an importance role for its normal function.

4.3. The cpSRP54 plays a central role in chloroplast development and photosynthetic pathways

The cpSRP54 protein is an essential component of the chloroplast-specific signal recognition particle (cpSRP) pathway, it forms a stable heterodimer with the chloroplast-specific cpSRP43 (Jeong *et al.* 2017). This heterodimer is responsible for targeting light-harvesting complex (LHC) proteins to the thylakoid membranes. This regulatory mechanism has been confirmed in *Arabidopsis*, rice, and cucumber (Zhang *et al.* 2022, 2025; Ji *et al.* 2023). However, whether the *cpSRP54* gene is related to other genes remains to be further investigated. In our study, PKH352, as a cpSRP54 mutant, serves as a valuable material for investigating the regulatory mechanism of cpSRP54. RNA-seq analysis comparing PKH352 and G42 revealed that a large number DEGs are associated with chloroplast development. Among these DEGs, the *LHC* gene was significantly upregulated in the mutant. This upregulation may be attributed to the cpSRP54 mutation impairing the transport of LHC proteins to thylakoids. Similarly, upregulation of *LHCs*

gene expression has also been observed in the yellowing mutant *R24* of pepper and the yellow-green leaf mutant *ygl9* of rice. Since LHC proteins are major components of the thylakoid membrane structure, the reduced content of LHC proteins on thylakoids results in developmental defects in the thylakoids of the PKH352 mutant. We also find genes such as *EGY1*, *EGY2*, *FTSH2*, and *FTSH12*, which are associated with chloroplast thylakoid membrane development, were significantly differentially expressed in the mutant (Figs. 5 and 6). These findings suggest that cpSRP54 may be involved in the regulation of these genes, similar to its role in regulating the *LHCs* gene. Additionally, GO enrichment analysis showed the DEGs were significantly enriched in the assembly process of photosystem I and photosystem II (Fig. 5-D). These findings indicate that cpSRP54 affects the expression of genes associated with these key photosynthetic pathways, which likely contributes to the significantly reduced photosynthetic capacity in the PKH352 mutant. Taken together, these results collectively indicate that cpSRP54 plays a critical role in chloroplast development and photosynthesis.

5. Conclusion

This study focused on investigating the watermelon material PKH352, which exhibits yellow-green coloration in its above-ground organs, accompanied by reduced chlorophyll content and lower maximal photochemical efficiency. Our findings revealed that this particular trait is closely associated with an irregular chloroplast structure at the molecular level, and its inheritance is governed by a single recessive gene, name *Clygp*. Using the map-based cloning method, *ClG42_04g0106300* as the candidate gene for *Clygp*, which encodes a signal recognition particle 54 kDa protein (cpSRP54). Further validation using a CRISPR/Cas9-mediated system confirmed that knockout of *ClG42_04g0106300* results in the yellow-green phenotype in watermelon. In addition, comparative transcriptomic analysis revealed that the *ClCG03G010030* gene plays a critical role in regulating chloroplast development and photosynthetic pathways modulating the expression of related genes.

Acknowledgements

This research was supported by the National Natural Science Foundation of China (32172602, 32472739), the Excellent Youth Foundation of Henan Scientific Committee, China (242300421030), and the Science and Technology Project of the Tibetan Plateau Seed Breeding Technology Innovation Center, China (LSQSCNYQ2025006). We thank Prof. Xingping Zhang and Prof. Yun Deng from the Peking University Institute of Advanced Agricultural Sciences for providing the mutant materials.

Declaration of competing interest

The authors declare that they have no conflict of interest.

Declaration of generative AI and AI-assisted technologies in the writing process

The authors declare that they did not use AI in the preparation and writing of this manuscript.

Data availability

The raw sequencing data were downloaded from the NCBI Sequence Read Archive (SRA) database (https://www.ncbi.nlm.nih.gov/sra) under accession number PRJNA1276008.

Appendices associated with this paper are available at https://doi.org/10.1016/j.jia.2025.11.013

References

Bischoff A, Ortelt J, Dünschede B, Zegarra V, Bedrunka P, Bange G, Schünemann D. 2024. The role of chloroplast SRP54 domains and its C-terminal tail region in post-and cotranslational protein transport *in vivo*. *Journal of Experimental Botany*, **75**, 5734–5749.

Cackett L, Luginbuehl L H, Schreier T B, LopezJuez E, Hibberd J M. 2021. Chloroplast development in green plant tissues: The interplay between light, hormone, and transcriptional regulation. *New Phytologist*, **233**, 2000–2016.

Cardona T, Shao S, Nixon P. 2018. Enhancing photosynthesis in plants: The light reactions. *Essays in Biochemistry*, **62**, 85–94.

Chen C J, Chen H, Zhang Y, Thomas H R, Frank M H, He Y H, Xia R. 2020. TBtools: An integrative toolkit developed for interactive analyses of big biological data. *Molecular Plant*, **13**, 1194–1202.

Chen F, Dong G J, Wu L M, Wang F, Yang X Z, Ma X H, Wang H L, Wu J H, Zhang Y L, Wang H Z, Qian Q, Yu Y C. 2016. A nucleus-encoded chloroplast protein YL1 is involved in chloroplast development and efficient biogenesis of chloroplast ATP synthase in rice. *Scientific Reports*, **6**, 32295.

Croce R, Carmo-Silva E, Cho Y B, Ermakova M, Harbinson J, Lawson T, McCormick A J, Niyogi K K, Ort D R, Patel-Tupper D, Pesaresi P, Raines C, Weber A P M, Zhu X. 2024. Perspectives on improving photosynthesis to increase crop yield. *Plant Cell*, **36**, 3944–3973.

Cutolo E A, Guardini Z, Dall'Osto L, Bassi R. 2023. A paler shade of green: Engineering cellular chlorophyll content to enhance photosynthesis in crowded environments. *New Phytologist*, **239**, 1567–1583.

Deng Y, Liu S C, Zhang Y L, Tan J S, Li X P, Chu X, Xu B H, Tian Y, Sun Y D, Li B S, Xu Y B, Deng X W, He H, Zhang X. 2022. A telomere-to-telomere gap-free reference genome of watermelon and its mutation library provide important resources for gene discovery and breeding. *Molecular Plant*, **15**, 1268–1284.

Dou J L, Yang H H, Sun D L, Yang S, Sun S R, Zhao S J, Lu X Q, Zhu H Y, Liu D M, Ma C S, Liu W G, Yang L M. 2022. The branchless gene *Clbl* in watermelon encoding a TERMINAL FLOWER 1 protein regulates the number of lateral branches. *Theoretical and Applied Genetics*, **135**, 65–79.

Duan S X, Guo Y M, Wang Y P, Umer M J, Liu D, Yang S, Niu H H, Sun S R, Yang L M, Dou J L, Zhu H Y. 2023. HD-Zip transcription factor is responsible for no-lobed leaf in watermelon (*Citrullus lanatus* L.). *Phyton-International Journal of Experimental Botany*, **18**, 1311–1328.

Fekih R, Takagi H, Tamiru M, Abe A, Natsume S, Yaegashi H, Sharma S, Sharma S, Kanzaki H, Matsumura H, Saitoh H, Mitsuoka C, Utsushi H, Uemura A, Kanzaki E, Kosugi S, Yoshida K, Cano L, Kamoun S, Terauchi R. 2013. MutMap^{+}: Genetic mapping and mutant identification without crossing in rice. *PLoS ONE*, **8**, e68529.

Gebremeskel H, Umer M J, Zhu H J, Li B B, Zhao S G, Yuan P L, Lu X Q, Nan H, Liu W G. 2023. Genetic mapping and molecular characterization of the delayed green gene *dg* in watermelon (*Citrullus lanatus*). *Frontiers in Plant Science*, **14**, 1152644.

He G, Zhang R, Jiang S H, Wang H H, Ming F. 2023. The MYB transcription factor RcMYB1 plays a central role in rose anthocyanin biosynthesis. *Horticulture Research*, **10**, uhad080.

Hristou A, Gerlach I, Stolle D S, Neumann J, Bischoff A, Dünschede B, Nowaczyk M M, Zoschke R, Schünemann D. 2019. Ribosome-associated chloroplast SRP54 enables efficient cotranslational membrane insertion of key photosynthetic proteins. *Plant Cell*, **31**, 2734–2750.

Hu L L, Zhang H Q, Xie C, Wang J, Zhang J Y, Wang H, Weng Y Q, Chen P, Li Y H. 2020. A mutation in CsHD encoding a histidine and aspartic acid domain-containing protein leads to *yellow young*

leaf-1 (*yyl-1*) in cucumber (*Cucumis sativus* L.). *Plant Science*, **293**, 110407.
Jeong J, Baek K, Kirst H, Melis A, Jin E. 2017. Loss of CpSRP54 function leads to a truncated light-harvesting antenna size in *Chlamydomonas reinhardtii*. *Biochimica et Biophysica Acta-Bioenergetics*, **1858**, 45–55.
Ji S L, Grimm B, Wang P. 2023. Chloroplast SRP43 and SRP54 independently promote thermostability and membrane binding of light-dependent protochlorophyllide oxidoreductases. *Plant Journal*, **115**, 1583–1598.
Ji S L, Siegel A, Shan S O, Grimm B, Wang P. 2021. Chloroplast SRP43 autonomously protects chlorophyll biosynthesis proteins against heat shock. *Nature Plants*, **7**, 1420–1432.
Kirst H, Melis A. 2014. The chloroplast signal recognition particle (CpSRP) pathway as a tool to minimize chlorophyll antenna size and maximize photosynthetic productivity. *Biotechnology Advances*, **32**, 66–72.
Lan Y H, Song Y, Zhao F, Cao Y, Luo D L, Qiao D R, Cao Y, Xu H. 2022. Phylogenetic, structural and functional evolution of the LHC gene family in plant species. *International Journal of Molecular Sciences*, **24**, 488.
Lei Y, Li B L, Wang X M, Wei J Y, Wang P Y, Zhao J, Yu F F, Qi Y F. 2023. Chloroplast SRP54 and FtsH protease coordinate thylakoid membrane-associated proteostasis in Arabidopsis. *Plant Physiology*, **192**, 2318–2335.
Levin G, Schuster G. 2023. LHC-like proteins: The guardians of photosynthesis. *International Journal of Molecular Sciences*, **24**, 2503.
Li C R, Du X J, Liu C M. 2025. Enhancing crop yields to ensure food security by optimizing photosynthesis. *Journal of Genetics and Genomics*, **52**, 1082–1095
Li Q L, Wang X M, Lei Y, Wang Y L, Li B L, Liu X Y, An L J, Yu F, Qi Y F. 2022. Chloroplast envelope ATPase PGA1/AtFtsH12 is required for chloroplast protein accumulation and cytosol-chloroplast protein homeostasis in Arabidopsis. *Journal of Biological Chemistry*, **298**, 102489.
Li W R, Zhang Y C, Mazumder M A R, Pan R H, Akhter D. 2022. Research progresses on rice leaf color mutants. *Crop Design*, **1**, 100015.
Lichtenthaler H K. 1987. Chlorophylls and carotenoids: Pigments of photosynthetic biomembranes. In: *Methods in Enzymology*. Academic Press, USA. pp. 350–382.
Liu D M, Liang J F, Liu Q Q, Chen Y X, Duan S X, Sun D L, Zhu H Y, Dou J L, Niu H H, Yang S, Sun S R, Hu J B, Yang L L. 2025. The pseudo-type response regulator gene *Clsc* regulates rind stripe coloration in watermelon. *Journal of Integrative Agriculture*, **24**, 147–160.
Liu D M, Yang H H, Yuan Y X., Zhu H Y, Zhang M J, Wei X C, Sun D L, Wang X J, Yang S, Yang L M. 2020. Comparative transcriptome analysis provides insights into yellow rind formation and preliminary mapping of the *Clyr* (*yellow rind*) gene in watermelon. *Frontiers in Plant Science*, **11**, 192.
Lu H J, Xiao Y Y, Liu Y X, Zhang J C, Zhao Y Y. 2024. Integrative transcriptomics and proteomics analysis of a cotton mutant *yl1* with a chlorophyll-reduced leaf. *Plants-Basel*, **13**, 1789.
Ma Y Y, Shi J C, Wang D J, Liang X, Wei F, Gong C M, Qiu L J, Zhou H C, Folta K M, Wen Y Q, Feng J Y. 2023. A point mutation in the gene encoding magnesium chelatase I subunit influences strawberry leaf color and metabolism. *Plant Physiology*, **192**, 2737–2755.
Naito Y, Hino K, Bono H, Ui-Tei K. 2015. CRISPR direct: Software for designing CRISPR/Cas guide RNA with reduced off-target sites. *Bioinformatics*, **31**, 1120–1123.
Neff M M, Turk E, Kalishman M. 2002. Web-based primer design for single nucleotide polymorphism analysis. *Trends in Genetics*, **18**, 613–615.
Niu H H, Li P F, Zhang M J, Meng H, Wang H, Yan W K, Liu D M, Dou J L, Yang S, Zhu H Y, Yang L M, He S. 2024. Genome-wide identification of *ClSPL* gene family and functional characterization of *ClSPL9* in watermelon. *Scientia Horticulturae*, **337**, 113539.
Pan J W, Song J, Sharif R, Xu X W, Li S T, Chen X H. 2024. A mutation in the promoter of the yellow stripe-like transporter gene in cucumber results in a yellow cotyledon phenotype. *Journal of Integrative Agriculture*, **23**, 849–862.
Rocha J J, Jayaram S A, Stevens T J, Muschalik N, Shah R D, Emran S, Robles C, Freeman M, Munro S. 2023. Functional unknomics: Systematic screening of conserved genes of unknown function. *Plos Biology*, **21**, e3002222.
Schünemann D. 2004. Structure and function of the chloroplast signal recognition particle. *Current Genetics*, **44**, 295–304.
Tang D D, Chen M J, Huang X H, Zhang G C, Zeng L, Zhang G S, Wu S J, Wang Y W. 2023. SRplot: A free online platform for data visualization and graphing. *PLoS ONE*, **18**, e0294236.
Walter B, Pieta T, Schünemann D. 2015. *Arabidopsis thaliana* mutants lacking cpFtsY or cpSRP54 exhibit different defects in photosystem II repair. *Frontiers in Plant Science*, **6**, 250.
Wang F, Duan S M, Tong L, Wang R N, Tao Y S. 2018. Fine mapping and candidate gene analysis of leaf color mutant in maize. *Journal of Plant Genetic Resources*, **6**, 1205–1209.
Wang L F, Sun J T, Wang C Y, Shangguan Z P. 2018. Leaf photosynthetic function duration during yield formation of large-spike wheat in rainfed cropping systems. *PeerJ*, **6**, e5532.
Wang Y, An Z, Li R, Yang X, Huang Y, Shao R, Ye Y. 2019. The nutritional status and fluorescence characteristics of maize cultivars with different chlorophyll content and yields. *Photosynthetica*, **57**, 295–302.
Yang J Y, Chen Y T, Sun X W, Zhang X Y, Wang S Y, Lyu Y P, Hu Y J, Wang X X. 2025. Curly leaf 1, a CHD domain-containing protein, regulates leaf development by H3K27me3 modification in rice. *The Crop Journal*, **2**, 360–371.
Yang S, Wang X J, Yan W K, Zhang Y, Song P Y, Guo Y M, Xie K X, Hu J B, Hou J, Wu Y F, Zhu H Y, Sun S R, Yang L M. 2023. Melon *yellow-green plant* (*Cmygp*) encodes a Golden2-like transcription factor regulating chlorophyll synthesis and chloroplast development. *Theoretical and Applied Genetics*, **136**, 66.
Yang S, Wang Y L, Zhu H Y, Zhang M J, Wang D K, Xie K X, Fan P F, Dou J L, Liu D M, Liu B, Chen C H, Yan Y, Zhao L J, Yang L M. 2022. A novel HD-Zip I/C2H2-ZFP/WD-repeat complex regulates the size of spine base in cucumber. *The New Phytologist*, **233**, 2643–2658.
Yang W Z, Yuan Y H, Yang P J, Li S Z, Ma S, Liu X Q, Zhou X J, Chen R M. 2023. ZmGluTR1 is involved in chlorophyll biosynthesis and is essential for maize development. *Journal of Plant Physiology*, **290**, 154115.
Yue L Q, Zhong M, Kang D J, Qin H Y, Li H C, Chai X, Kang Y Y, Yang X. 2024. Genome-wide identification and characterization of flavonol synthase (*FLS*) gene family in *Brassica* vegetables and their roles in response to biotic and abiotic stresses. *Scientia Horticulturae*, **331**, 113168.
Zhang C, Zhang J X, Tang Y J, Liu K W, Liu Y, Tang J Q, Zhang T, Yu H X. 2021. DEEP GREEN PANICLE1 suppresses GOLDEN2-LIKE activity to reduce chlorophyll synthesis in rice glumes. *Plant Physiology*, **185**, 469–477.
Zhang R X, Zhang N N, Wang Y X, Abid K, Shuai M A, Bai X, Zeng Q, Pan Q M, BaoHua L, Zhang L G. 2023. Blue light induces leaf color change by modulating carotenoid metabolites in orange-head chinese cabbage (*Brassica rapa* L. ssp. *pekinensis*). *Journal of Integrative Agriculture*, **22**, 3296–3311.
Zhang T Q, Xiao W W, Wang Z W, Zhang J C, Shen W Q, Tu R R, Wu R H, Zhou K, Sang X C, Ling Y H, He G H, Zhang T. 2025. YGL9 mediates LHC assembly by regulating LHCPs transport and chlorophyll synthesis in rice. *Plant Journal*, **121**, e17256.
Zhang T T, Dong X Y, Yuan X, Hong Y Y, Zhang L L, Zhang X, Chen S X. 2022. Identification and characterization of *CsSRP43*, a major gene controlling leaf yellowing in cucumber. *Horticulture Research*, **9**, uhac212.
Zhao M H, Li X, Zhang X X, Zhang H, Zhao X Y. 2020. Mutation mechanism of leaf color in plants: A review. *Forests*, **11**, 851.
Zhu H Y, Zhang M J, Sun S R, Yang S, Li J X, Li H, Yang H H, Zhang K G, Hu J B, Liu D M, Yang L M. 2019. A single nucleotide deletion in an ABC transporter gene leads to a dwarf phenotype in watermelon. *Frontiers in Plant Science*, **10**, 1399.
Zhu Y C, Yuan G P, Wang Y F, An G L, Li W H, Liu J P, Sun D X. 2022. Mapping and functional verification of leaf yellowing genes in watermelon during whole growth period. *Frontiers in Plant Science*, **13**, 1049114.